Modeling of lithium granule injection in NSTX with M3D-C1

A. Fil [c,*], E. Kolemen [c], A. Bortolon [b], N. Ferraro [b], S. Jardin [b], P.B. Parks [a], R. Lunsford [b], R. Maingi [b]

[a] *General Atomics, PO Box 85608, San Diego, CA 92186, USA*
[b] *Princeton Plasma Physics Laboratory, Princeton, NJ 08543, USA*
[c] *Princeton University, NJ 08540, USA*

ABSTRACT

In this paper we present initial simulations of pedestal control by Lithium Granule Injection (LGI) in NSTX. A model for small granule ablation has been implemented in the M3D-C1 code [1], allowing the simulation of realistic Lithium granule injections. 2D simulations in NSTX L-mode and H-mode plasmas are done and the effect of granule size, injection angle and velocity on the pedestal gradient increase are studied. For H-mode cases, the amplitude of the local pressure perturbation caused by the granules is highly dependent on the solid granule size. In our simulations, reducing the granule injection velocity allows one to inject more particles at the pedestal top.

© 2017 The Authors. Published by Elsevier Ltd.
This is an open access article under the CC BY-NC-ND license.
(http://creativecommons.org/licenses/by-nc-nd/4.0/)

1. Introduction

Real-time pedestal control is a crucial topic for future fusion reactors such as ITER where the pedestal has to be kept free of Edge-Localized-Modes (or ELMs) for heat flux management and stationary against many perturbations. It is also crucial to maintain high plasma performance. Many different control schemes have been developed and tested to adjust and regulate the pedestal at DIII-D and other devices. NSTX-U plans to do additional tests. In particular, gas puffing [2] injects fuel or impurities at the plasma edge to control the plasma pedestal density, 3D magnetic perturbations [3] create an edge stochastic layer thus increasing the transport (which lowers the pedestal pressure gradient), Lithium Granule Injections (LGI) [4] induce pressure perturbations triggering ELMs and can thus change the ELM frequency and their impact on the Plasma Facing Components (PFCs). All these techniques aim at changing the pedestal parameters to mitigate ELMs. The final aim of this work would be to combine all these methods in an adaptive and automatic pedestal control algorithm for tokamaks. Such a capability could allow one to explore new innovative scenarios such as the Super H-Mode [5] or lithium induced ELM-free regimes [6]. In order to reach this goal, it is important to understand the physics bases for how the different control actuators affect the pedestal. This is especially important in order to evaluate applicability to future reactors, e.g. ITER.

In this paper, we focus on the LGI technique and present numerical simulations with the M3D-C1 code. M3D-C1 [1] is a state-of-the-art 3D full-MHD code with realistic geometry and is being developed to study plasma response when several actuators are triggered (gas puffing, 3D magnetic perturbations and LGI). Experimentally, high frequency Li granule injections have been performed in DIII-D plasmas [7] and a LGI system has recently been installed on NSTX-U. As it is using non-fuel, non-recycling materials, LGI allows a decoupling of ELM control from plasma fueling. DIII-D experiments have demonstrated robust ELM-pacing and a triggering efficiency higher than 80% for 0.9 mm lithium granules, but some concern exists because of the variability of triggered-ELM sizes. In particular, in high density, low-torque ITER baseline scenarios, an increase of the ELM frequency by LGI-pacing did not directly translate in ELM size mitigation [8]. Modeling with M3D-C1 has the potential to investigate these phenomena by simulating the non-linear, 3 dimensional dynamic evolution of a realistic tokamak equilibrium subject to a triggered ELM. Prior to this work, M3D-C1 did not possess any LGI model. Studies of LGI with M3D-C1, whose first steps are detailed in this paper, will improve our physical understanding of this method and will allow us to build reduced models for control applications.

In this paper, we first present the implementation of granule ablation models in M3D-C1. We will then present the results of 2D NSTX LGI simulations which investigate the pressure perturbation triggered by different granule sizes, injection angle and velocity.

---

* Corresponding author.
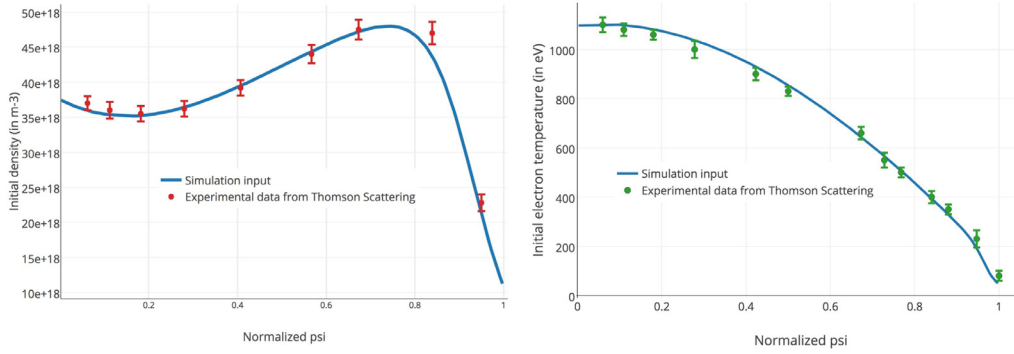 *E-mail address:* afil@pppl.gov (A. Fil).

Fig. 1. Midplane pressure and density profiles before firing a Lithium Granule in NSTX.

Table 1
Range of granule input parameters used in the simulations.

r_p (mm)	Inj. velocity (m/s)	Ablation cloud radius (cm)	Inj. angle (degrees)
0.2–1	50–200	1–5	− 70 to + 70

2. Modeling of lithium granule injection in M3D-C1

Two models have been implemented in the code M3D-C1 to calculate the ablation rate of the lithium granule. The first one [9,10] is a Neutral Gas Shielding Model calibrated on DIII-D experimental measurements of lithium granules ablation rates. The second one [11] is valid for small size granules (sub-mm) where the contribution of plasma ions to the granule ablation is not negligible. In this model, the ablation flow is treated as an expanding monoatomic gas with spherical symmetry, and a realistic Maxwellian distribution function for incident fast electrons is used. Moreover, the model accounts for slowing down and pitch-angle scattering collisions of these fast electrons with cloud atoms.

In both cases, the granule is modeled as a varying Gaussian density source multiplied by the normalized ablation rate A_r. The width of the source is defined by the realistic granule radius r_p multiplied by an arbitrary parameter. This parameter allows one to change the size of the ablation cloud to match what is experimentally observed. Note that this is the only "free" parameter of the granule model and that experimentally its value is imprecise (between 5 and 100 times the solid granule radius). Its impact on the simulations will be discussed in Section 3.

The granule ablation rate is calculated at each time-step as $A_r = C(n_e, T_e, r_p) \times X_m$, where r_p is the granule radius and (n_e, T_e) are the electron density and temperature of the back- ground plasma at the granule position. $C(n_e, T_e, r_p)$, the non-dimensional ablation coefficient, depends on the species parameter and is determined by solving the gas dynamic equations for the ablation flow for each set of (r_p, n_e, T_e). A function fitting these results is used in M3D-C1. X_m is the usual law used for strongly shielded cryogenic pellets. The granule ra- dius r_p and thus the source width is decreasing as the granule is ablated by the plasma, as $\frac{\delta r_p}{\delta t} = -C(n_e, T_e, r_p) \times X_p$. More details on the model can be found in [10,11].

3. Results

The 2D simulations (axisymmetric) presented in this paper start from experimental NSTX equilibrium, electron density and temperature profiles. The target plasma is an ELMy H-mode (plasma discharge 129,015) [6] with temperature measurements from the Thomson Scattering system, during the inter-ELM period. Fig. 1
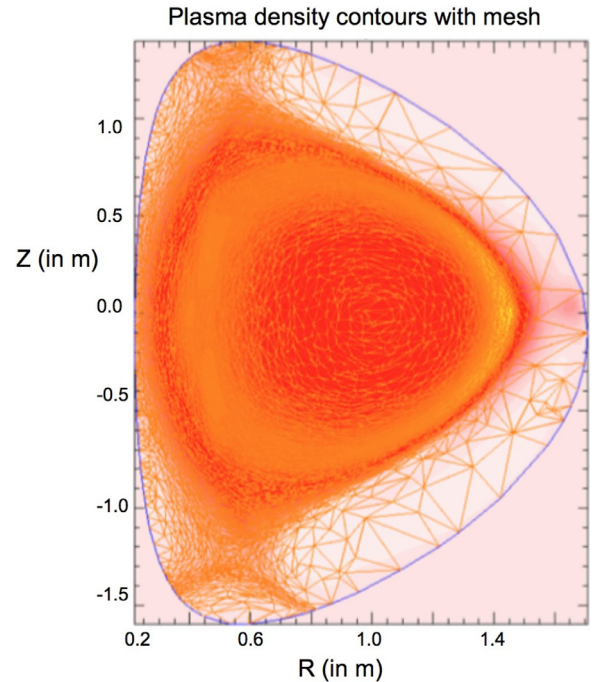

Fig. 2. Poloidal cross section of the plasma showing the mesh used in the simulations.

shows the experimental data and the fits which are used as the simulations initial profiles.

The main parameters are $B_T = 0.44$ T, $I_p = 0.785$ MA, $a = 0.627$ m. The simulation is initiated at 0.4 s from the beginning of the discharge, within an inter-ELM time interval. The separatrix is at $R = 1.48$ m and the top of the pressure pedestal is at $R = 1.46$ m at that moment (see Fig. 4). A series of simulations were performed of injections with different radius, initial speed, injection angle and size of the ablation cloud, as summarized in Table 1: Typical meshes sizes are 1–5 mm and the time step is $10^{-8} - 10^{-7}$ s.

A typical mesh used in these simulations is shown Fig. 2. In M3D-C1, meshing zones can be defined and the meshing is usually tuned with the Simmodeler software. In this case, we choose a fine mesh around the separatrix.

Overall, it takes between 0.2 and 3ms for the pellet to fully ablate, consistent with experimental values [7]. Comparing to previous L-mode simulations [12], the penetration depth and the ablation time is up to one order of magnitude shorter due to the higher electron density and temperature in H-mode.
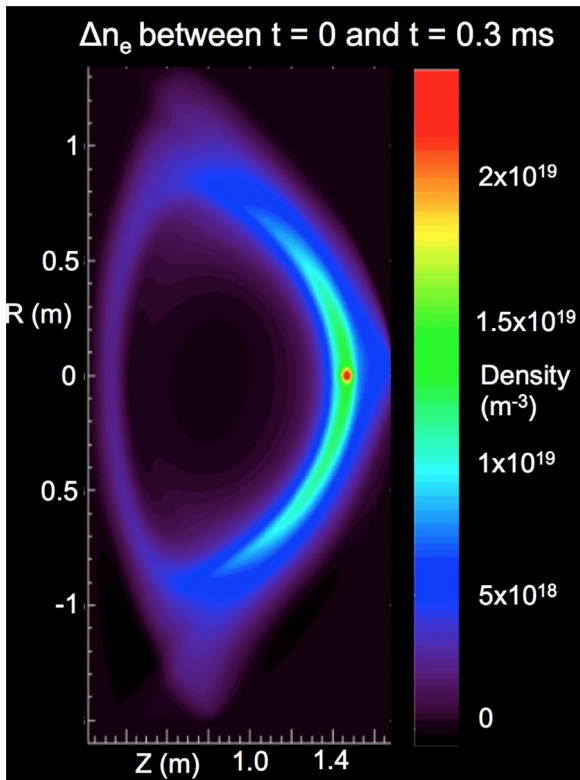
Fig. 3. Poloidal cross section of the density increase due to the injection of a 0.8 mm granule in a NSTX H-mode plasma. Difference of the density between the start of the injection and $t = 300\,\mu s$ after the injection.

In these simulations, the granule starts propagating inward at $R = 1.5$ m with a constant velocity. When entering the plasma, the granule generates a large and localized density increase as can be seen in Fig. 3. On a short timescale, electron conduction along the field lines reheats this high density region and leads to a localized plasma pressure increase. An example of pressure increase due to the injection of a 0.8 mm granule is shown in Fig. 4. A pressure increase is also found in the Scrape-Of-Layer (SOL), which is associated to the boundary conditions used in the open field lines region, thus keeping the temperature constant even when the density increases.

Fig. 5 shows the number of ablated atoms injected in the simulations. The larger granules achieve a significantly larger penetration depth, up to 7 cm for 1 mm granules at 100 m/s, i.e. 3 cm inside the pedestal top. Fig. 5 also shows that while the number of particles locally deposited at the pedestal top is higher for large granules, they also inject a large number of particles inside the separatrix. These values are very close to the experimental ones presented in [7] and [9]. The associated pressure increase at maximum ablation is displayed in Fig. 6, showing that larger granules create a commensurately larger increase in the pressure gradient.

The initial velocity at which the granule is injected also changes the penetration depth and the particle deposition as can be seen on Fig. 7. For this particular case, slower granules deposit more particles at the pedestal top and also lead to a smaller fueling. The associated pressure increase at maximum ablation is presented on Fig. 8 and shows that the pressure perturbation is lower for the fast granules compared to the slower ones. Note here that these are qualitative results as the current model does not include effects arising from the non-uniformity of the magnetic field, which may decelerate the granule. These effects will be included and tested in future work.

The angle of injection can also decrease the penetration depth as can be seen on Fig. 9. This figure presents the injection of a 1 mm granule in NSTX H-mode with varying angles of injection. No significant differences have been observed between upward and downward injections. Injecting with an angle α with a velocity V_{inj} is also very similar to injecting with no angle at a velocity of $\cos(\alpha) \times V_{inj}$.

Finally, the impact of the size of the ablation cloud has been tested. Three simulations have been performed, injecting granules
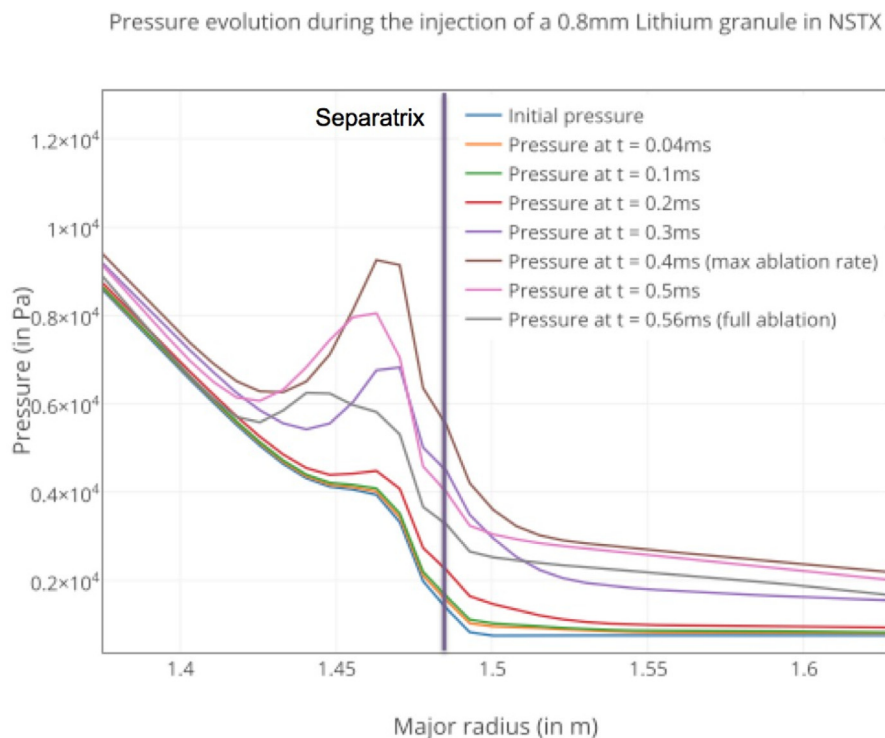

Fig. 4. Successive pressure profiles at the poloidal plan where the granule is injected. A large increase of the pedestal pressure is observed.

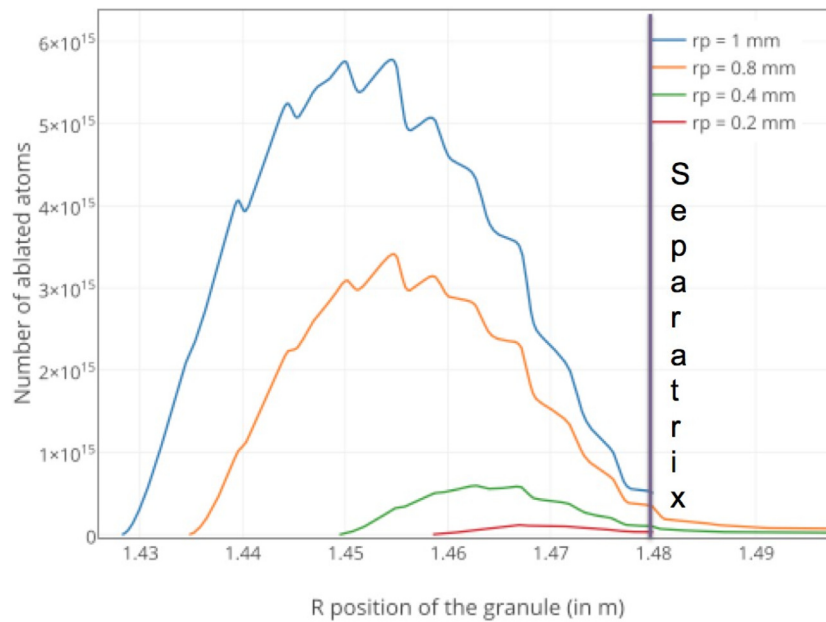Number of particles injected for different granule sizes

Fig. 5. Number of ablated atoms injected as the granule is penetrating into the plasma. The top of the pressure pedestal is at $R = 1.46$ m for this NSTX discharge, and the seperatrix at $R = 1.48$ m.
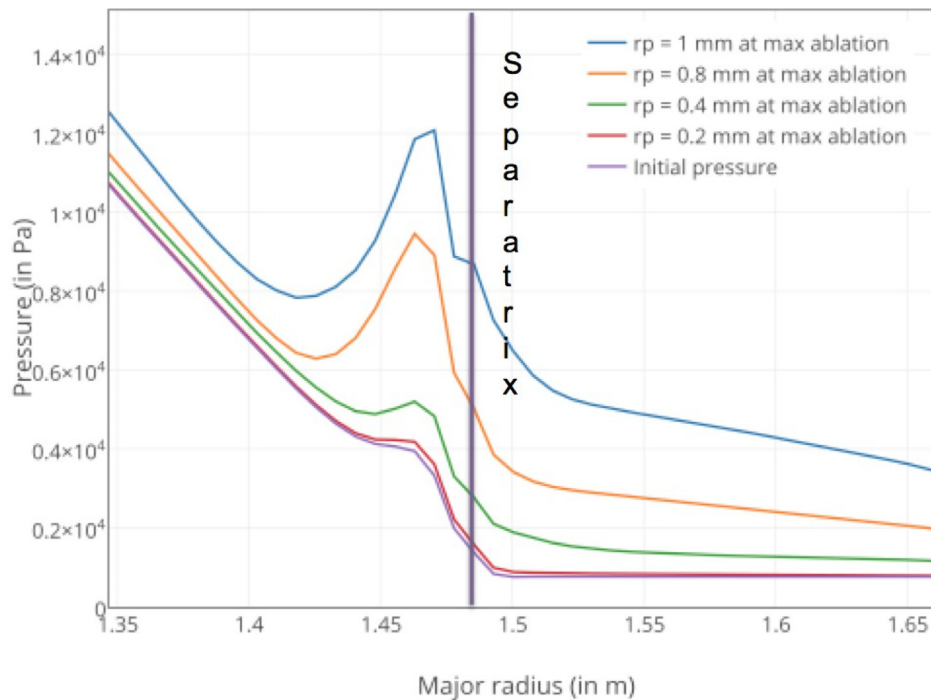

Fig. 6. Pressure profile at maximum ablation for different granule sizes rp.

of the same size (i.e. same number of particles and ablation rate) but with a wider source, i.e. larger ablation cloud. The lower value (1 cm) is determined by numerical limitations of the current grid. In our simulations, the density increase is larger for small width sources, but within the range tested (1–5 cm) it has a small impact (few %) on the maximum induced pressure perturbation. Note that this is the radial width of the source which is varied here. The effect of the toroidal width of the source will be tested in future 3D simulations.

4. Discussion and perspectives

These simulations show that the local pressure perturbation at the pedestal induced by LGI increases with granule size and decreases with velocity. To avoid an undesirable decrease of the temperature inside the separatrix, one can inject granules with a larger injection angle or by decreasing the injection velocity.

A LGI system has just been installed on NSTX-U and synthetic diagnostics (line integrated measurement of density from
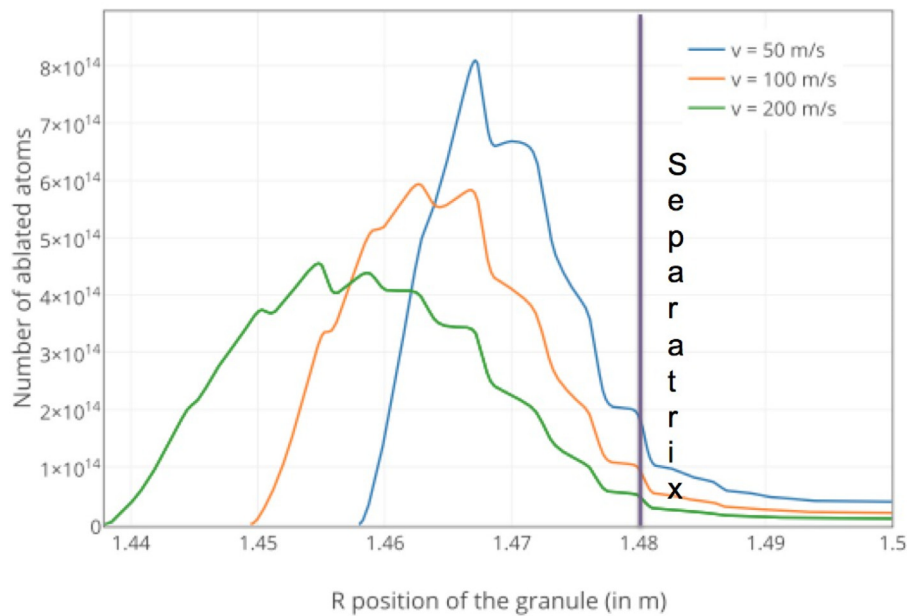
Number of particles injected for different injection velocities (rp = 0.4mm)

Fig. 7. Number of ablated atoms injected when the granule is penetrating into the plasma. Injection of a 0.4 mm granule with different velocities. The top of the pressure pedestal is at $R = 1.46$ m for this NSTX discharge.
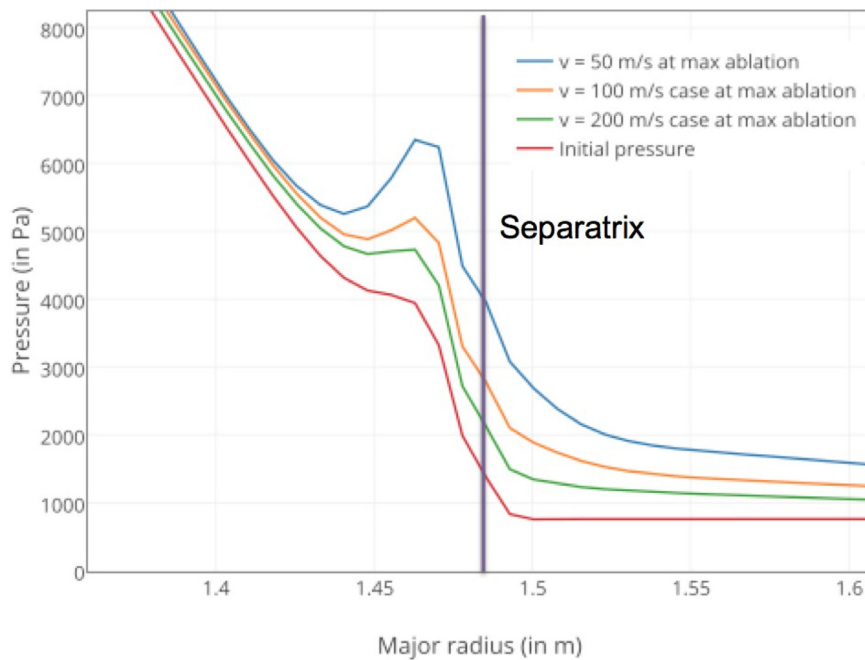

Fig. 8. Pressure profile at maximum ablation for different injection velocities.

interferometry, heat-flux footprint in vicinity of the strike-points) are currently being implemented in M3D-C1. This will allow us to compare the predicted density increase at the edge to the measured values.

The simulations presented in this paper are 2D and thus lack the physics ingredients essential to the destabilization of MHD modes such as ELMs. These are simulations using few computing nodes and which allow to validate our granule model. We can already affirm that the local pressure threshold for ELM triggering will be reached more easily by utilizing large granules. Moreover, granules with a high injection velocity are not found to be

always beneficial. A fast granule might increase the pedestal pressure gradient very quickly, but to values below the ELM-triggering threshold, when slower granules might increase the pedestal gradient above this threshold for the same number of injected particles.

Realistic 3D simulations will need much more computing power than the 2D simulations presented in this paper. However, they are crucial if one wants to study the impact of the pressure perturbation on the MHD activity, as well as the toroidal dynamic of the granule cloud. These 3D simulations are on-going and aim at specifying quantitatively this threshold and the impact of granule
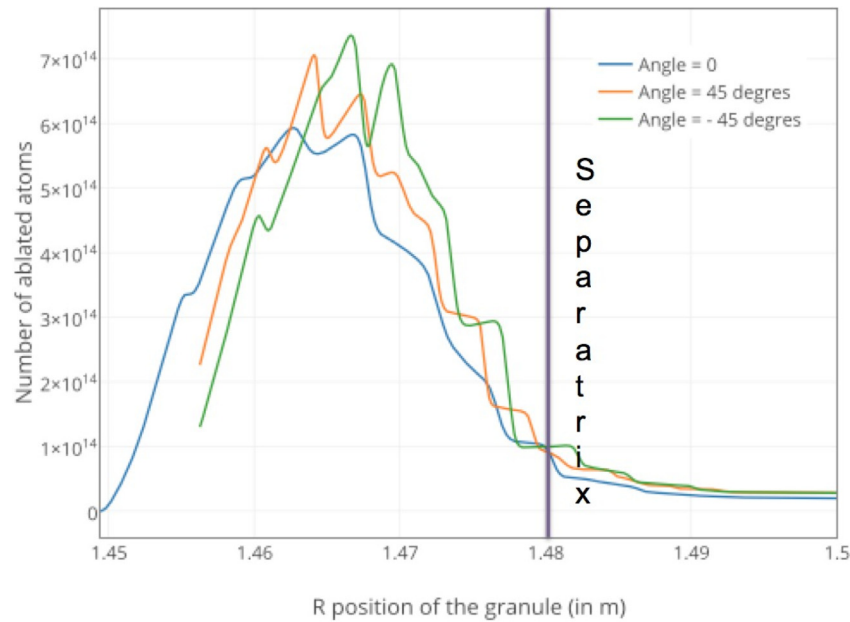
Fig. 9. Number of ablated atoms injected as the granule is penetrating into the plasma. Injection of a 0.4 mm granule with different injection angles (Midplane injection corresponds to 0°). The top of the pressure pedestal is at $R = 1.46$ m for this NSTX discharge.

parameters on ELM properties. These simulations aim at finding an effective compromise between fast ELM-pacing and high confinement. Mesh adaptation, mesh packing techniques and high-order 3D finite elements are used to allow simulation of sub-mm granules (as is already the case in 2D), without constraints on the granule toroidal width. Grad B effects on the granule velocity are also being implemented and their effects will be investigated.

The digital data for this paper can be found in http://arks.princeton.edu/ark:/88435/dsp018p58pg29j.

References

[1] S.C. Jardin, et al., Comput. Sci. Discovery 5 (2012) 014002.
[2] R. Nazikian, et al., in: Proceedings of IAEA, 2014 EX1-1.
[3] R.J. Hawryluk, et al., Nucl. Fusion 55 (2015) 053001.
[4] D.K. Mansfield, et al., Nucl. Fusion 53 (2013) 113023.
[5] W.M. Solomon, et al., PRL 113 (2014) 135001.
[6] R. Maingi, et al., PRL 103 (2009) 075001.
[7] A. Bortolon, et al., Nucl. Fusion 56 (2016) 056008.
[8] A. Bortolon, et al., in: Proceeding of the 22nd PSI conference, 2016.
[9] R. Lunsford, et al., Fusion Eng. Des. (2016).
[10] P.B. Parks, et al., Nucl. Fusion 34 (417) (1994).
[11] P.B. Parks, private communication.
[12] A. Fil, et al., Proceeding of the 57th Annual Meeting of the APS Division of Plasma Physics.